Comprehensive Proteomic Profiling of Exfoliation Glaucoma Via Mass Spectrometry Reveals SVEP1 as a Potential Biomarker

Jiayong Li,[1,2] Yuncheng Ma,[2] Lingling Xie,[2] Kaichen Zhuo,[1,2] Yuxian He,[1,2] Xin Ma,[1,2] Shufen Zheng,[3,4] Shicheng Guo,[5] Yizhen Tang,[6] Guzainuer Muhetaer,[2] Mireayi Aizezi,[2] Dan Zhang,[2] Aizezi Wumaier,[2] Xu Zhang,[7] Chao Tang,[8] Wei Wang,[1] Wenyong Huang,[1] and Xinbo Gao[1,2]

[1]State Key Laboratory of Ophthalmology, Zhongshan Ophthalmic Center, Sun Yat-Sen University, Guangdong Provincial Key Laboratory of Ophthalmology and Vision Science, Guangdong Provincial Clinical Research Center for Ocular Diseases, Guangzhou, China
[2]Department of Ophthalmology, the First People's Hospital of Kashi Prefecture (The Affiliated Kashi Hospital of Sun Yat-Sen University), Kashi, China
[3]Center for Intelligent Medicine Research, Greater Bay Area Institute of Precision Medicine (Guangzhou), Guangzhou, China
[4]Center for Evolutionary Biology, Intelligent Medicine Institute, School of Life Sciences, Fudan University, Shanghai, China
[5]School of Life Sciences, Fudan University, Shanghai, China
[6]Department of Ophthalmology, Beijing Tongren Hospital, Capital Medical University, Beijing Ophthalmology and Visual Sciences Key Laboratory, Beijing, China
[7]Center for Reproductive Medicine, Women and Children's Hospital of Chongqing Medical University, Center for Reproductive Medicine, Chongqing Health Center for Women and Children, Chongqing Reproductive Genetics Institute, Chongqing, China
[8]National Clinical Research Center for Child Health of the Children's Hospital, Zhejiang University School of Medicine, Hangzhou, China

Correspondence: Xinbo Gao, State Key Laboratory of Ophthalmology, Zhongshan Ophthalmic Center, Sun Yat-Sen University, No. 7 Jinsui Rd., Tianhe District, Guangzhou 510623, China; gaoxb@mail.sysu.edu.cn.
Wenyong Huang, State Key Laboratory of Ophthalmology, Zhongshan Ophthalmic Center, Sun Yat-Sen University, No. 54 Xianlie South Rd., Yuexiu District, Guangzhou 510060, China; huangwenyong@gzzoc.com.

Received: October 9, 2024
Accepted: January 29, 2025
Published: March 7, 2025

Citation: Li J, Ma Y, Xie L, et al. Comprehensive proteomic profiling of exfoliation glaucoma via mass spectrometry reveals SVEP1 as a potential biomarker. *Invest Ophthalmol Vis Sci.* 2025;66(3):19. https://doi.org/10.1167/iovs.66.3.19

Purpose. This study investigated the proteomic landscape of exfoliation glaucoma to find potential biomarkers.

Methods. The study enrolled 34 patients diagnosed with either exfoliation syndrome with/without glaucoma or age-related cataract. Plasma proteins were analyzed through mass spectrometry and Mendelian randomization (MR) based on data from deCODE, FinnGen, Atherosclerosis Risk in Communities (ARIC), eQTLGen, and UK Biobank (UKB) cohorts to infer relationships.

Results. Among 2025 plasma proteins analyzed, 130 were differentially expressed in the exfoliation glaucoma group, which exhibited elevated intraocular pressure. Our proteomics data suggested that infection, immune responses including intestinal immune network, endocrine hormones, and complement and coagulation cascades are involved in the development of exfoliation glaucoma. Notably, there was a significant correlation between SVEP1 and exfoliation glaucoma (odds ratio [OR] = 1.20, 95% confidence interval [CI] = 1.10 to 1.31, $P = 0.0000428$), with findings corroborated in an independent cohort. Further analysis predicted a protective role of LOXL1-AS1 in exfoliation glaucoma through its regulation of SVEP1 expression. In MR phenome-wide association studies, SVEP1 was associated with complications of exfoliation glaucoma. After multiple testing corrections, there was a tendency for SVEP1 to be associated with glaucoma (OR = 1.14, 95% CI = 1.11 to 1.16, $P = 0.0000003$) and type 2 diabetes (OR = 1.07, 95% CI = 1.05 to 1.08, $P = 0.0000067$).

Conclusions. Plasma proteomic analysis reveals that high expression of SVEP1 is a risk factor for exfoliation glaucoma, which potentially affects diabetes and is affected by estradiol or LOXL1-AS1. However, further research is needed to establish causality.

Keywords: proteomics, exfoliation glaucoma (XFG), Mendelian randomization (MR), SVEP1, PheWAS, LOXL1-AS1

Glaucoma, as a neurodegeneration disease, is the leading cause of irreversible blindness globally affecting approximately 95 million people, thus early detection and effective treatment are essential.[1] Exfoliation glaucoma (XFG), the predominant cause of secondary glaucoma, associated with principal susceptibility gene lysyl oxidase like 1 (LOXL1), appears to have worse prognosis.[1,2] XFG is the ocular manifestation of exfoliation syndrome (XFS), which is a systemic disease associated with increased risk of vascular disease.[3,4] In addition, the polymorphisms in the long non-coding RNA LOXL1-antisense 1 (LOXL1-AS1) is a risk factor for XFG.[5] However, it is still unclear what the underlying mechanisms of XFG are. Therefore, we need the results of further experimental and clinical studies to elucidate the potential pathophysiological processes of XFG.

Recently, human plasma proteomics, the key biomarkers for diagnosis and prognosis in precision medicine, have made great achievements, such as the maturation of new high-throughput technologies and updates of the Human Plasma Proteome Project (HPPP).[6] In recent years, there are many researches about plasma protein and eye disease. By investigating the plasma proteomics, it is beneficial for us to understand the mechanism of XFG pathogenesis. Moreover, Mendelian randomization (MR) is a robust computational methodology that uses single nucleotide polymorphisms (SNPs) from quantitative trait loci (QTL) and genome-wide association studies (GWAS) summary statistics to analyze relationships between exposures and outcomes.[7]

Here, we aimed to identify comprehensive plasma proteome profiling of XFG by the data-independent acquisition mass spectrometer (DIA-MS). With the proteomics data, we analyzed plasma proteins significantly associated with incident XFG by our observational studies and the biologic processes and pathways of these proteins regarding XFG pathogenesis. Furthermore, we explored the relationships between specific proteins and diseases by the MR approach, and the potential mechanisms led to XFG. In addition, we conducted an MR phenome-wide association study (MR-PheWAS) and a review of current studies of biomarkers for XFG in plasma or serum. Consequently, we undertook an integrated analysis of observational and genetic data of proteins that could serve as potential drug targets, providing new insights for the clinical prevention and treatment of XFG.

Methods

Study Approval

The First People's Hospital of Kashi Prefecture Ethics Committee approved this study that was conducted in accordance with the guidelines of the Declaration of Helsinki. This article does not contain identifiable data for any participant. All publicly available summarized GWAS data sources in this study were approved by the respective institutional ethics committees. We summarized the methodological framework in Figure 1.

Patients and Specimens

In total, we collected 34 blood samples of patients with XFS and age-related cataract (ARC) controls between February and May in 2023 in the First People's Hospital of Kashi Prefecture in Northwest China which were categorized as follows: XFG ($n = 10$), XFS ($n = 12$), and ARC ($n = 12$). All patients were admitted to the hospital for surgery on similar dates. The inclusion criteria are described in the Supplementary Methods.

Blood samples were collected after the patients' overnight fasting under routine clinical blood guidance using Vacutainer K2 EDTA tubes (Becton Dickinson, Franklin Lakes, NJ, USA). We centrifuged blood samples at 2000 relative centrifugal force (rcf) for 15 minutes at 4°C after clotting at room temperature and then immediately aliquoted and

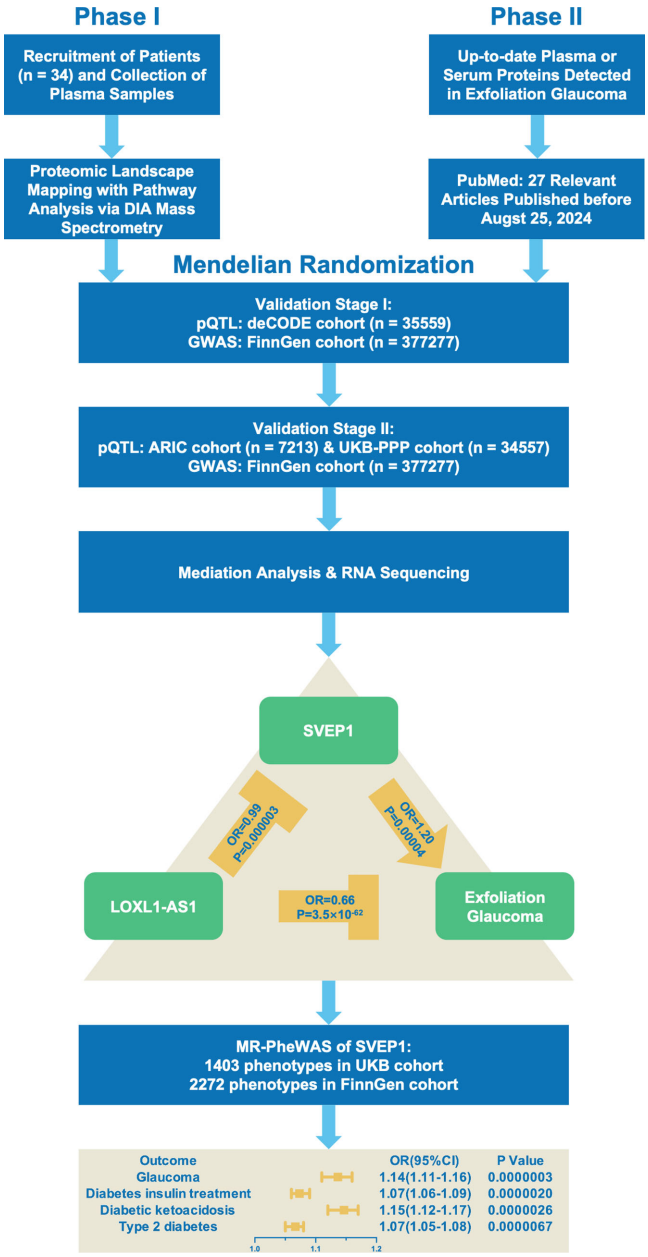

Figure 1. Flowchart of the identification and integration of the differentially expressed proteins by DIA-MS and MR. ARIC = Atherosclerosis Risk in Communities Study; DIA-MS = data-independent acquisition mode mass spectrometry; LOXL-AS1 = lysyl oxiase-like 1 antisense RNA 1; MR = Mendelian randomization; OR = odds ratio; PheWAS = Phenome-Wide Association Studies; pQTL = protein quantitative trait locus; SVEP1 = Sushi, von Willebrand factor type A, EGF and pentraxin domain containing 1; UKB-PPP = UKB Pharma Proteomics Project.

stored plasma into sterile centrifuge tubes at −80°C for future analysis.

Data-Independent Acquisition Mode Mass Spectrometry Analysis

We lysed plasma samples with Dissolution Buffer lysis buffer (8 M Urea, 100 mM triethylammonium bicarbonate; Sigma/T7408-500ML, pH 8.5) and then centrifuged the samples at 12,000 g for 15 minutes at 4°C and the supernatant was reduced with 1M DL-Dithiothreitol (Sigma/D9163-25G) for 1 hour at 56°C, and subsequently alkylated with sufficient iodoacetamide (Sigma/I6125-25G) for 1 hour at room temperature in the dark followed by an ice-bath for 2 minutes. After protein quality test (described in the Supplementary Methods), we performed tryptic digestion at 37°C for 4 hours and then added trypsin (Promega/V5280) and $CaCl_2$ for digesting overnight. We mixed formic acid with the digested sample, adjusted pH < 3, and centrifuged at 12,000 g for 5 minutes at room temperature. We loaded the supernatant to the C18 desalting column slowly, washed with washing buffer (0.1% formic acid and 3% acetonitrile) 3 times, then we added elution buffer (0.1% formic acid and 70% acetonitrile). We collected and lyophilized the eluents of each sample. We dissolved the lyophilized powder using 0.1% formic acid, centrifuged at 14,000 g for 20 minutes at 4°C, and injected 200 ng of the supernatant sample into the sample for liquid-quality detection.

We used a Vanquish Neo upgraded ultra-HPLC (UHPLC) system with a C18 pre-column of 174500 (5 mm × 300 µm, 5 µm, thermo) heated at 50°C in a column oven, and a C18 analytical column of ES906 (PepMap TM Neo UHPLC 150 µm × 15 cm, 2 µm, thermo), an Orbitrap Astral mass spectrometer (Thermo Fisher Scientific, USA) in Novogene Co. Ltd. using DIA and an Easy-spray ion (ESI) source with the ion spray voltage 1.9 kilovolt (kV), the ion transfer tube temperature was 290°C, and a full first-stage mass spectrometry scanning range of m/z 380 to 980. The elution conditions of the liquid chromatography were as shown in the Supplementary Methods.

We set the primary MS resolution to 240,000 (200 m/z), AGC to 500%, the parent ion window size to 2-Th, the number of DIA windows to 300, the NCE to 25%, the secondary m/z acquisition range from 150 to 2000, the sub-ion resolution Astral to 80000, and the maximal injection time was 3 ms.

The mass spectrometry detection raw files (Project ID: IPX0008349000, submitted at iProX[8,9]) were searched and analyzed using the DIA-NN library search software. More details are described in the Supplementary Methods.

Statistics

Protein quantification results were statistically analyzed using the *t*-test, and if the data were found not to follow a normal distribution, then the Mann-Whitney *U* test was used instead. Differentially expressed proteins (DEPs) were defined as those with significant quantitative differences between the case and control groups ($P < 0.05$, fold change > 1.2 or fold change < 0.83). The comparison among groups was performed using the Chi-square test, Kruskal–Wallis tests, or 1-way ANOVA.

Pathway/Network Analysis

We performed comprehensive functional analysis using the Gene Ontology (GO) and InterPro (IPR) databases through the InterProScan program. Additionally, we utilized the Clusters of Orthologous Groups (COG) and Kyoto Encyclopedia of Genes and Genomes (KEGG) databases to investigate protein families and pathways. The DEPs were used for volcano plot analysis, cluster heatmap analysis, and enrichment analysis of GO, IPR, Gene Set Enrichment Analysis (GSEA), and KEGG terms. The protein-protein interaction (PPI) analysis network was established by the Search Tool for the Retrieval of Interacting Genes (STRING) database and was visualized via Cytoscape. In addition, we used GOsemsim to predict the key proteins.[10]

Data Source

We used protein QTL (pQTL) in the deCODE and UK Biobank Pharma Proteomics Project (UKB-PPP) cohort for discovery study and then the cohort of Atherosclerosis Risk in Communities (ARIC) study for replication validation.[11–13] In addition, we used *cis*-expression QTL(eQTL) summary statistics from the eQTLGen Consortium.[14] We used microbiota quantitative trait loci (mbQTL) of genus Senegalimassilia from the MiBioGen consortium.[15,16] We obtained GWAS summary statistics about XFG, POAG, ARC, and other cataracts from the DF9 release of the FinnGen Study.[17] More details are described in the Supplementary Methods.

Mendelian Randomization

We used a bidirectional two-sample MR approach. We excluded the palindromic or ambiguous SNP. The SNPs with potential confounding factors ($P < 5 \times 10^{-8}$) were screened by the Gene ATLAS database (http://geneatlas.roslin.ed.ac.uk/phewas/).[18] We used the inverse variance weighted (IVW) method as our primary source of MR estimates, and when the number of inverse variances (IVs) was only one, we used the Wald ratio instead of the IVW method. We selected the one with the lowest *P* value for the following analysis if different SOMAmers or Olink antibodies shared the same pQTL.[19] More details are described in the Supplementary Methods.

Sensitivity Analysis

We performed sensitivity analyses using complementary approaches that are robust to violation of MR assumptions, including MR Egger intercept test and Mendelian Randomization Pleiotropy RESidual Sum and Outlier test (MR-PRESSO) to evaluate the potential presence of horizontal pleiotropy. In addition, a leave-one-out analysis was conducted to assess the influence of potentially pleiotropic IVs on the estimates. We also used the Radial MR method to detect outliers and repeated MR analysis after excluding outliers. We analyzed Steiger filtering directionality test to explore the robustness of the effect direction. The Cochran's Q heterogeneity test was used to test the heterogeneity between casual estimates. The strength of the IVs was evaluated with F statistics, whereas if the value of the F statistic was > 10 it was considered that there was no significant weak instrumental bias of the estimates.

Investigative Ophthalmology & Visual Science

Mediation Analysis

We used a mediation analysis to investigate the effect of an exposure variable on an outcome variable through a mediating variable. We initially extracted relevant coefficients and standard errors from two separate datasets. To ensure consistency in our analysis, we only included effect sizes calculated using the IVW method. We calculated Mediated Effect = $\text{Coefficient}_{\text{Exposure-Mediator}} \times \text{Coefficient}_{\text{Mediator-Outcome}}$, and further calculated the Z-score = mediated effect/ standard error of the mediated effect. If $P = 2 \times$ (1-normal distribution cumulative probability function at $|Z|$) was less than 0.05, the mediated effect was considered significant.

RNA-Sequencing of the LOXL1-AS1/SVEP1 Pathway

We collected and analyzed the data of RNA-sequencing from a previous study that contained a LOXL1-AS1 targeted siRNA knockdown model and an overexpression model built by vectors carrying LOXL1-AS1, Δ14-LOXL1-AS1, or the compliment sequence, pENTR1A plasmids containing the LOXL1 promoter, which were transfected into immortalized human lens epithelial (HLE-B3) cells.[20]

Mendelian Randomization Phenome-Wide Association Study

To identify comorbidities caused by SVEP1, we performed an MR-PheWAS using phenome-wide association study summary statistics based on the UKB cohort and the FinnGen cohort (R9). The UK Biobank data supplied 1403 electronic health record (EHR)-derived International Classification of Diseases (ICD)-based phenotypes for 20 million imputed variants in 400,000 White British individuals (https://pheweb.org/UKB-SAIGE/).[21] In addition, the FinnGen data (R9) supplied 2272 phenotypes. In the MR analysis, we used the IVW method as the main outcome indicator and $P < 0.05$ for the IVW method was suggested for the nominal significant. Furthermore, we used multiple testing corrections and considered $P < 0.05/3675$ as a threshold to determine the statistical significance.

Results

Clinical Characteristics of Patients

Our study included 34 patients without significant differences in age, gender, body mass index, and axial length (Supplementary Table S1). The median IOP at XFG was 28 millimeters of mercury (mm Hg) (interquartile range [IQR] = 26 to 42) was highest ($P < 0.001$), whereas in XFS it was 17 mm Hg (IQR = 15 to 18 mm Hg) and in ARC it was 16 mm Hg (IQR = 15 to 20 mm Hg). The median cornea endothelial cell density at XFG was 1847 mm^2 (IQR = 1752 to 2043), and was the lowest ($P = 0.013$), whereas in XFS it was 2222 mm^2 (IQR = 2145 to 2508), and in ARC it was 2328 mm^2 (IQR = 2265 to 2577).

Plasma Proteomic Landscape of XFG/XFS

We identified 1668 proteins in XFG, 1738 proteins in XFS, and 1734 proteins in ARC (Fig. 2A). In total, we identified 2025 proteins which were distributed at approximately 7 orders of magnitude in plasma (range from 0.011 to 440,000 ng/mL), which included 717 protein biomarkers (Human Disease Plasma Protein Biomarker Database, online at http://biokb.ncpsb.org.cn/hdpp/#/) and according to Human Protein Atlas version 23.0 (https://www.proteinatlas.org/) 594 low abundance proteins (< 10 ng/mL) of 1319 proteins matched with the HPPP (Fig. 2B, Supplementary Table S2).[22] The heatmap showed the protein xpression characteristics of each group (Fig. 2C). We found 1339 proteins between XFG and XFS (43 upregulated and 38 downregulated DEPs; Supplementary Table S3, Supplementary Fig. S1A), 1317 proteins between XFG and ARC (36 upregulated and 62 downregulated DEPs; Supplementary Table S4, Supplementary Fig. S1B) and 1362 proteins between XFS and ARC (27 upregulated and 55 downregulated DEPs; Supplementary Table S5, Supplementary Fig. S1C). Comparing XFS and ARC, 130 proteins were differentially expressed in the XFG group, which exhibited elevated intraocular pressure.

Comparing XFG and XFS, the top 5 upregulated DEPs were protein HEG homolog 1, transforming growth factor beta-1 proprotein, immunoglobulin kappa variable 1D-33, immunoglobulin kappa variable 1–33, and dynein heavy chain 11, axonemal, whereas the top 5 downregulated DEPs were cDNA FLJ51597, highly similar to C4b-binding protein alpha chain, serum amyloid P-component, transthyretin, properdin, and cDNA FLJ58124, highly similar to complement factor I (Fig. 3A). In addition, four low abundance DEPs (fibroblast growth factor receptor 4, mannosyl-oligosaccharide 1,2-alpha-mannosidase IC, eukaryotic translation initiation factor 5, and protocadherin Fat 2) were detected (Fig. 3B).

Comparing XFG and ARC, the top 5 upregulated DEPs were dynein heavy chain 11, axonemal, immunoglobulin kappa variable 1D-33, B cell receptor heavy chain variable region (Fragment), cadherin-13, and uncharacterized protein DKFZp779H1622 (fragment), whereas the top 5 downregulated DEP were Ig heavy chain variable region (fragment 1), Ig heavy chain variable region (fragment 2), glutamate dehydrogenase 2, mitochondrial, alpha globin, and putative hydroxypyruvate isomerase (Fig. 3C). In addition, 8 low abundance DEPs (fibroblast growth factor receptor 4, eukaryotic translation initiation factor 5, protocadherin, EGF-containing fibulin-like extracellular matrix protein 2, ATP synthase subunit alpha, mitochondrial, eukaryotic initiation factor 4A-I, T-complex protein 1 subunit delta, and enoyl-CoA hydratase domain-containing protein 2, mitochondrial) were detected (Fig. 3D).

Comparing XFS and ARC, the top 5 upregulated DEPs were apolipoprotein F, APOB protein, lysosome-associated membrane glycoprotein 1, 14-3-3 protein gamma, and apolipoprotein L1 (fragment), whereas the top 5 downregulated DEPs were protein HEG homolog 1, Ig heavy chain variable region (fragment 1), Ig heavy chain variable region (fragment 2), ribonuclease pancreatic, and glutaminyl-peptide cyclotransferase (see Fig. 3E). In addition, 6 low abundance DEPs (antileukoproteinase, integral membrane protein 2B, C-C motif chemokine 18, actin-related protein 2/3 complex subunit 5, glutaminyl-peptide cyclotransferase, and exportin-2) were detected (Fig. 3F).

To evaluate the expression trend of proteins in different degrees of the disease, we then performed a series test of clusters for all significant DEPs in groups XFG, XFS, and ARC (Fig. 2D, Table 1). The proteins were classified into 6 clusters, wherein the Sushi, von Willebrand factor type A, EGF, and pentraxin domain-containing protein 1 (SVEP1; see Fig. 3C), transforming growth factor beta-1 proprotein,

Investigative Ophthalmology & Visual Science

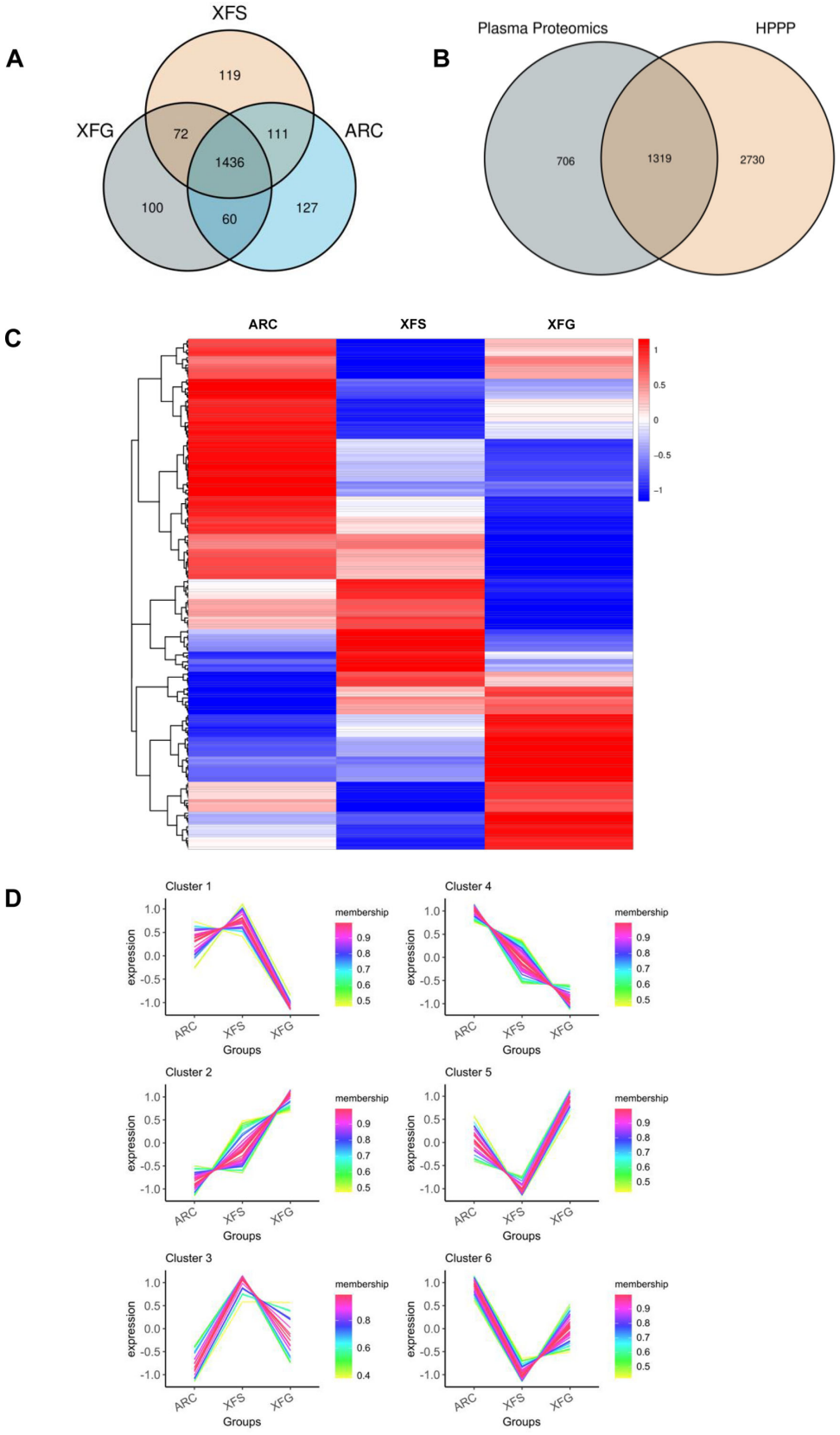

Figure 2. Plasma proteome determined by DIA-MS. (**A**) Venn diagram analysis of the number of plasma proteins in groups XFG, XFS, and ARC detected by DIA-MS. (**B**) Venn diagram analysis of the proteins identified by DIA-MS compared with the HPPP database. (**C**) Heatmap of the identified proteins in groups XFG, XFS, and ARC. (**D**) Series test of cluster for all significantly differentially expressed proteins in groups XFG, XFS, and ARC. ARC = age-related cataract; DIA-MS = data-independent acquisition mode mass spectrometry; HPPP = Human Plasma Proteome Project; XFG = exfoliation glaucoma; XFS = exfoliation syndrome.

Investigative Ophthalmology & Visual Science

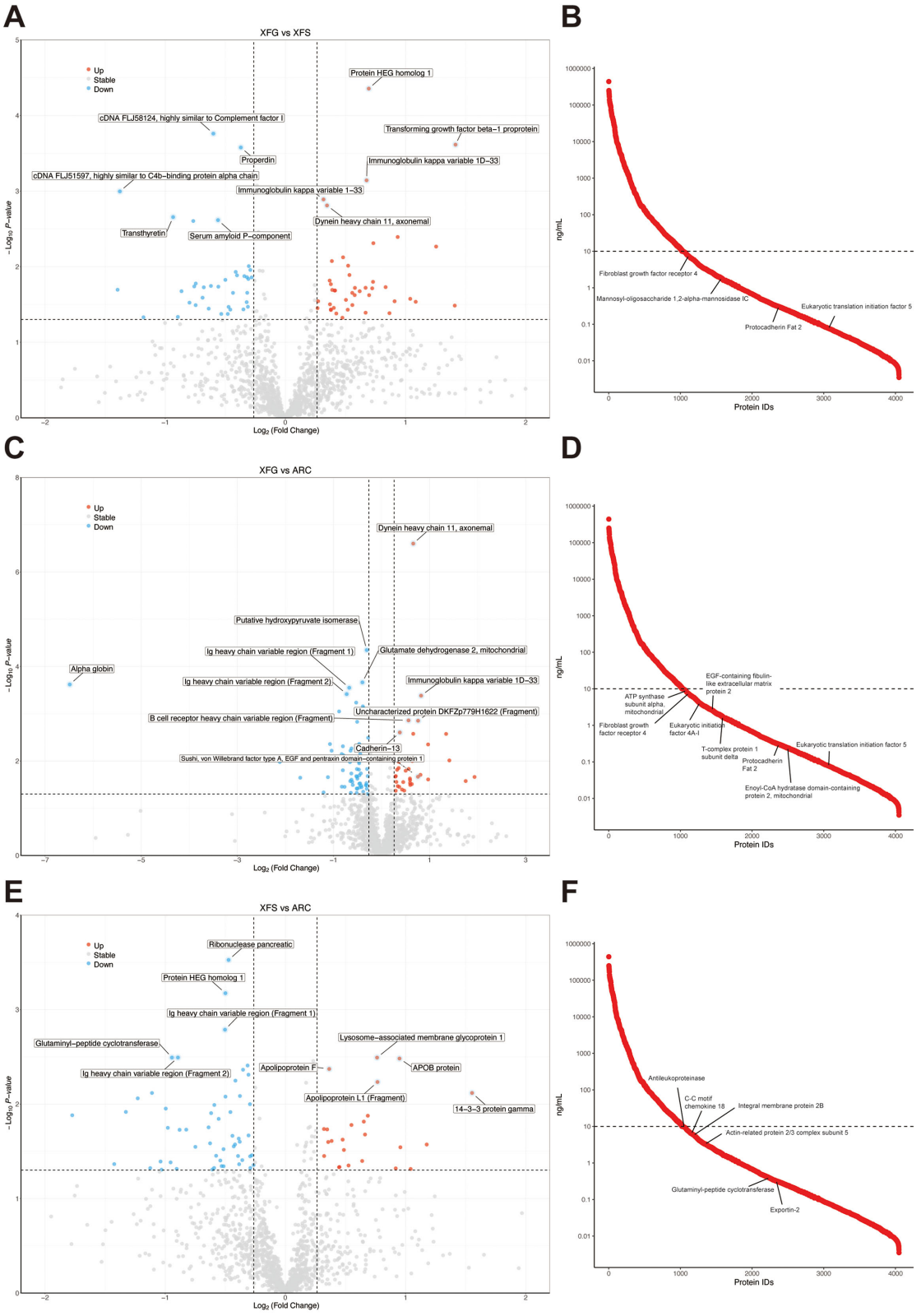

Figure 3. Analysis of the differentially expressed proteins identified by DIA-MS. (**A**) The significance of differentially expressed proteins between groups XFG and XFS. (**B**) Low-abundance proteins identified between groups XFG and XFS. (**C**) The significance of differentially expressed proteins between groups XFG and ARC. (**D**) Low-abundance proteins identified between groups XFG and ARC. (**E**) The significance of differentially expressed proteins between groups XFS and ARC. (**F**) Low-abundance proteins identified between groups XFS and ARC.ARC = age-related cataract; DIA-MS = data-independent acquisition mode mass spectrometry; XFG = exfoliation glaucoma; XFS = exfoliation syndrome.

Investigative Ophthalmology & Visual Science

Table 1. Series Test of Cluster for all Significantly Differentially Expressed Proteins

Protein	Description	Gene	Cluster
A0A024R884	Tenascin C (Hexabrachion), isoform CRA_a	TNC	1
A0A075B7B8	Immunoglobulin heavy variable 3/OR16-12 (non-functional) (fragment)	IGHV3OR16-12	1
A0A087WSX0	Immunoglobulin lambda variable 5-45	IGLV5-45	1
A0A0B4J1Y9	Immunoglobulin heavy variable 3-72	IGHV3-72	1
A0A0C4DGB6	Serum albumin	ALB	1
A0A1L2BU33	Anti-staphylococcal enterotoxin D heavy chain variable region (fragment)		1
A0A1W6IYJ0	N90-VRC38.03 heavy chain variable region (fragment)		1
A0A2U8J8X8	Ig heavy chain variable region (fragment)	IgH	1
A8K5T0	cDNA FLJ75416, highly similar to Homo sapiens complement factor H (CFH), mRNA		1
B4DRF2	cDNA FLJ58124, highly similar to complement factor I		1
B4E1D8	cDNA FLJ51597, highly similar to C4b-binding protein alpha chain		1
P00740	Coagulation factor IX	F9	1
P02743	Serum amyloid P-component	APCS	1
P02766	Transthyretin	TTR	1
P03951	Coagulation factor XI	F11	1
P06276	Cholinesterase	BCHE	1
P13716	Delta-aminolevulinic acid dehydratase	ALAD	1
P14209	CD99 antigen	CD99	1
P19827	Inter-alpha-trypsin inhibitor heavy chain H1	ITIH1	1
P27918	Properdin	CFP	1
P43251	Biotinidase	BTD	1
P43652	Afamin	AFM	1
P53634	Dipeptidyl peptidase 1	CTSC	1
Q5EFE5	Anti-RhD monoclonal T125 gamma1 heavy chain		1
Q6ZP85	cDNA FLJ26301 fis, clone DMC07540		1
Q8NBP7	Proprotein convertase subtilisin/kexin type 9	PCSK9	1
Q9NPH3	Interleukin-1 receptor accessory protein	IL1RAP	1
Q9NR34	Mannosyl-oligosaccharide 1,2-alpha-mannosidase IC	MAN1C1	1
Q9NYQ8	Protocadherin fat 2	FAT2	1
A0A023T424	MHC class I antigen (fragment)	HLA-B	2
A0A075B6I1	Immunoglobulin lambda variable 4-60	IGLV4-60	2
A0A0F7T891	IGHV5-51 protein (fragment)	IGHV5-51	2
A0A0U4DJF7	Haptoglobin (fragment)	HP	2
A0A1C9J6R5	B cell receptor heavy chain variable region (fragment)		2
A0A2U8J8H9	Ig heavy chain variable region (fragment)	IgH	2
A0A2U8J8Q2	Ig heavy chain variable region (fragment)	IgH	2
A0A2U8J9C7	Ig heavy chain variable region (fragment)	IgH	2
B3KWB5	cDNA FLJ42722 fis, clone BRAMY4000277, highly similar to Alpha-1B-glycoprotein		2
B4DHZ6	Transferrin, isoform CRA_c	TF	2
O95967	EGF-containing fibulin-like extracellular matrix protein 2	EFEMP2	2
P01137	Transforming growth factor beta-1 proprotein	TGFB1	2
P01593	Immunoglobulin kappa variable 1D-33	IGKV1D-33	2
P02679	Fibrinogen gamma chain	FGG	2
P02750	Leucine-rich alpha-2-glycoprotein	LRG1	2
P02763	Alpha-1-acid glycoprotein 1	ORM1	2
P07602	Prosaposin	PSAP	2
P07900	Heat shock protein (HSP) 90-alpha	HSP90AA1	2
P0C0L5	Complement C4-B	C4B	2
P17066	Heat shock 70 kDa protein 6	HSPA6	2
P22455	Fibroblast growth factor receptor 4	FGFR4	2
P25705	ATP synthase subunit alpha, mitochondrial	ATP5F1A	2
P40197	Platelet glycoprotein V	GP5	2
P55290	Cadherin-13	CDH13	2
P60842	Eukaryotic initiation factor 4A-I	EIF4A1	2
P61981	14-3-3 protein gamma	YWHAG	2
Q13477	Mucosal addressin cell adhesion molecule 1	MADCAM1	2
Q14643	Inositol 1,4,5-trisphosphate receptor type 1	ITPR1	2
Q14651	Plastin-1	PLS1	2
Q4LDE5	Sushi, von Willebrand factor type A, EGF, and pentraxin domain-containing protein 1	SVEP1	2
Q53FD7	Nucleoporin 54kDa variant (fragment)		2
Q68DR3	Uncharacterized protein DKFZp779H1622 (fragment)	DKFZp779H1622	2
Q6GMW4	IGL @ protein	IGL @	2
Q8J008	Protein C (fragment)	PROC	2
Q96DT5	Dynein heavy chain 11, axonemal	DNAH11	2
Q96SN8	CDK5 regulatory subunit-associated protein 2	CDK5RAP2	2

Investigative Ophthalmology & Visual Science

Table 1. Continued

Protein	Description	Gene	Cluster
Q9UL93	Myosin-reactive immunoglobulin heavy chain variable region (fragment)		2
A0A0G2JMI3	Immunoglobulin heavy variable 1-69-2	IGHV1-69-2	3
A0A1B2FK72	Apolipoprotein L1 (fragment)	APOL1	3
A0A1L2BU39	Anti-staphylococcal enterotoxin E heavy chain variable region (fragment)		3
B2RBZ5	cDNA, FLJ95778, highly similar to Homo sapiens serpin peptidase inhibitor, clade A (alpha-1 antiproteinase, antitrypsin), member 10 (SERPINA10), mRNA		3
O43505	Beta-1,4-glucuronyltransferase 1	B4GAT1	3
P01705	Immunoglobulin lambda variable 2-23	IGLV2-23	3
P02810	Salivary acidic proline-rich phosphoprotein 1/2	PRH1	3
P03973	Antileukoproteinase	SLPI	3
P04745	Alpha-amylase 1	AMY1A	3
P0C0L4	Complement C4-A	C4A	3
P11279	Lysosome-associated membrane glycoprotein 1	LAMP1	3
P22392	Nucleoside diphosphate kinase B	NME2	3
P55060	Exportin-2	CSE1L	3
Q10588	ADP-ribosyl cyclase/cyclic ADP-ribose hydrolase 2	BST1	3
Q13790	Apolipoprotein F	APOF	3
Q5SRP5	Apolipoprotein M	APOM	3
Q7Z7Q0	APOB protein	APOB	3
Q8IYE1	Coiled-coil domain-containing protein 13	CCDC13	3
Q9H804	cDNA FLJ14022 fis, clone HEMBA1003538, weakly similar to COMPLEMENT C1R COMPONENT		3
Q9UIB8	SLAM family member 5	CD84	3
Q9Y5P4	Collagen type IV alpha-3-binding protein	COL4A3BP	3
V9HWI6	Epididymis secretory protein Li 51	HEL-S-51	3
A0A068LKQ8	Ig heavy chain variable region (fragment)		4
A0A0F7T983	IGHV1-2 protein (fragment)	IGHV1-2	4
A0A0K2BMD8	Mutant hemoglobin alpha 2 globin chain	HBA2	4
A0A0X9TDD0	GCT-A1 light chain variable region (fragment)		4
A0A0X9V981	MS-A2 light chain variable region (fragment)		4
A0A109PP82	MS-C2 light chain variable region (fragment)		4
A0A125U0V4	GCT-A2 heavy chain variable region (fragment)		4
A0A1L2BU38	Anti-staphylococcal enterotoxin E heavy chain variable region (fragment)		4
A0A2U8J8D6	Ig heavy chain variable region (fragment)	IgH	4
A0A2U8J8T2	Ig heavy chain variable region (fragment)	IgH	4
A0A2U8J8Y8	Ig heavy chain variable region (fragment)	IgH	4
A0A2U8J8Z8	Ig heavy chain variable region (fragment)	IgH	4
A0A2U8J904	Ig heavy chain variable region (fragment)	IgH	4
A0A2U8J944	Ig heavy chain variable region (fragment)	IgH	4
A0A2U8J954	Ig heavy chain variable region (fragment)	IgH	4
A0A2U8J967	Ig heavy chain variable region (fragment)	IgH	4
A0A2U8J984	Ig heavy chain variable region (fragment)	IgH	4
A0A2U8J9A2	Ig heavy chain variable region (fragment)	IgH	4
A0A2Y9CYE4	Ig heavy chain variable region (fragment)	IgH	4
A0A3B3ISR2	Complement C1r subcomponent	C1R	4
A2NXP9	K light chain variable region (fragment)		4
A2NZ55	Variable immunoglobulin anti-estradiol heavy chain (fragment)		4
B4DZ36	cDNA FLJ58441, highly similar to Attractin		4
G3V1N2	HCG1745306, isoform CRA_a	HBA2	4
P01040	Cystatin-A	CSTA	4
P01709	Immunoglobulin lambda variable 2-8	IGLV2-8	4
P01766	Immunoglobulin heavy variable 3-13	IGHV3-13	4
P01877	Immunoglobulin heavy constant alpha 2	IGHA2	4
P02746	Complement C1q subcomponent subunit B	C1QB	4
P04211	Immunoglobulin lambda variable 7-43	IGLV7-43	4
P06732	Creatine kinase M-type	CKM	4
P0CG47	Polyubiquitin-B	UBB	4
P11597	Cholesteryl ester transfer protein	CETP	4
P35443	Thrombospondin-4	THBS4	4
P49448	Glutamate dehydrogenase 2, mitochondrial	GLUD2	4
P49913	Cathelicidin antimicrobial peptide	CAMP	4
P50991	T-complex protein 1 subunit delta	CCT4	4
P55010	Eukaryotic translation initiation factor 5	EIF5	4
Q5T013	Putative hydroxypyruvate isomerase	HYI	4

Investigative Ophthalmology & Visual Science

Table 1. Continued

Protein	Description	Gene	Cluster
Q6GMX0	Uncharacterized protein		4
Q6N096	Uncharacterized protein DKFZp686I15196	DKFZp686I15196	4
Q86YB7	Enoyl-CoA hydratase domain-containing protein 2, mitochondrial	ECHDC2	4
Q86YQ4	Alpha-1 globin (fragment)	HBA1	4
Q8N5F4	IGL @ protein	IGL @	4
Q8NHQ9	ATP-dependent RNA helicase DDX55	DDX55	4
Q96SB0	Anti-streptococcal/anti-myosin immunoglobulin lambda light chain variable region (fragment)		4
Q9Y6R7	IgGFc-binding protein	FCGBP	4
S6C4S2	IgG L chain		4
V9H1D9	Alpha globin		4
A0A2Q2TTZ9	Immunoglobulin kappa variable 1-33	IGKV1D-33	5
A0A2U8J8N7	Ig heavy chain variable region (fragment)	IgH	5
A0A2U8J931	Ig heavy chain variable region (fragment)	IgH	5
A2N0T6	VH6DJ protein (fragment)	VH6DJ	5
A2N2F5	VL4 protein (fragment)	VL4	5
B2RBS8	cDNA, FLJ95666, highly similar to Homo sapiens albumin (ALB), mRNA		5
O75015	Low affinity immunoglobulin gamma Fc region receptor III-B	FCGR3B	5
P01854	Immunoglobulin heavy constant epsilon	IGHE	5
P08493	Matrix Gla protein	MGP	5
P09211	Glutathione S-transferase P	GSTP1	5
P23470	Receptor-type tyrosine-protein phosphatase gamma	PTPRG	5
P25774	Cathepsin S	CTSS	5
P34096	Ribonuclease 4	RNASE4	5
P41222	Prostaglandin-H2 D-isomerase	PTGDS	5
P61769	Beta-2-microglobulin	B2M	5
Q12841	Follistatin-related protein 1	FSTL1	5
Q14126	Desmoglein-2	DSG2	5
Q16627	C-C motif chemokine 14	CCL14	5
Q16769	Glutaminyl-peptide cyclotransferase	QPCT	5
Q68DL7	Uncharacterized protein C18orf63	C18orf63	5
Q7Z3Y4	Uncharacterized protein		5
Q8WWZ8	Oncoprotein-induced transcript 3 protein	OIT3	5
Q9UBX5	Fibulin-5	FBLN5	5
Q9UHI6	Probable ATP-dependent RNA helicase DDX20	DDX20	5
Q9ULI3	Protein HEG homolog 1	HEG1	5
S6B2A6	IgG H chain		5
S6B2C3	IgG L chain		5
S6C4R2	IgG H chain		5
S6C4R7	IgG L chain		5
A0A0B4J1V2	Immunoglobulin heavy variable 2-26	IGHV2-26	6
A0A0B4J2B8	Immunoglobulin heavy variable 1/OR15-9 (non-functional) (fragment)	IGHV1OR15-9	6
A0A0F7SZ86	IGHV2-70 protein (fragment)	IGHV2-70	6
A0A120HF66	IBM-A1 heavy chain variable region (fragment)		6
A0A1W6IYK3	N90-VRC38.10 light chain variable region (fragment)		6
A0A2U8J8B6	Ig heavy chain variable region (fragment)	IgH	6
A0A2U8J940	Ig heavy chain variable region (fragment)	IgH	6
A0A2U8J947	Ig heavy chain variable region (fragment)	IgH	6
A0A2U8J973	Ig heavy chain variable region (fragment)	IgH	6
A0A2U8J9A4	Ig heavy chain variable region (fragment)	IgH	6
A0A2U8J9A6	Ig heavy chain variable region (fragment)	IgH	6
A0A2Y9CYF7	Ig heavy chain variable region (fragment)	IgH	6
A2J1N3	Rheumatoid factor RF-IP20 (fragment)		6
A2JA16	Anti-mucin1 light chain variable region (fragment)		6
A2JA19	Anti-mucin1 light chain variable region (fragment)		6
A2NB43	Cold agglutinin FS-1 H-chain (fragment)	IGH@	6
A2NB45	Cold agglutinin FS-1 L-chain (fragment)		6
O15511	Actin-related protein 2/3 complex subunit 5	ARPC5	6
P00746	Complement factor D	CFD	6
P01814	Immunoglobulin heavy variable 2-70	IGHV2-70	6
P07333	Macrophage colony-stimulating factor 1 receptor	CSF1R	6
P07998	Ribonuclease pancreatic	RNASE1	6
P08637	Low affinity immunoglobulin gamma Fc region receptor III-A	FCGR3A	6
P0DP02	Immunoglobulin heavy variable 3-30-3	IGHV3-30-3	6

Investigative Ophthalmology & Visual Science

Table 1. Continued

Protein	Description	Gene	Cluster
P0DP08	Immunoglobulin heavy variable 4-38-2	IGHV4-38-2	6
P19320	Vascular cell adhesion protein 1	VCAM1	6
P24592	Insulin-like growth factor-binding protein 6	IGFBP6	6
P27105	Erythrocyte band 7 integral membrane protein	STOM	6
P55774	C-C motif chemokine 18	CCL18	6
Q12805	EGF-containing fibulin-like extracellular matrix protein 1	EFEMP1	6
Q14118	Dystroglycan	DAG1	6
Q15063	Periostin	POSTN	6
Q7Z379	Uncharacterized protein DKFZp686K04218 (fragment)	DKFZp686K04218	6
Q8TER0	Sushi, nidogen and EGF-like domain-containing protein 1	SNED1	6
Q9HCU0	Endosialin	CD248	6
Q9NPY3	Complement component C1q receptor	CD93	6
Q9UL89	Myosin-reactive immunoglobulin heavy chain variable region (fragment)		6
Q9Y287	Integral membrane protein 2B	ITM2B	6

transferrin (isoform CRA_c), heat shock protein (HSP) 90-alpha, heat shock 70 kDa protein 6, complement C4-B, and protein C (fragment) were categorized in cluster 2 (the levels of proteins increased as the disease worsened). In addition, anti-staphylococcal enterotoxin E heavy chain variable region (fragment), cathelicidin antimicrobial peptide, complement C1r subcomponent, complement C1q subcomponent subunit B, variable immunoglobulin anti-estradiol heavy chain (fragment), cystatin-A, cholesteryl ester transfer protein, thrombospondin-4, and glutamate dehydrogenase 2 (mitochondrial) were in cluster 4 (the levels of proteins decreased as the disease worsened).

To compare with the results in previous plasma/serum proteome study, we searched in PubMed on August 25, 2024, by searching the texts filtered by (pseudoexfoliation glaucoma) OR (pseudoexfoliation syndrome) OR (exfoliative glaucoma) OR (pseudoexfoliative glaucoma) OR (exfoliation syndrome) OR (exfoliation glaucoma) AND (protein* OR proteom*) and published before August 25, 2024. We manually reviewed all 516 results and there remained 27 articles related to plasma/serum protein assays for XFG/XFS (Table 2).

Pathway/Network Analysis

The three most significant biological process categories identified in the GO enrichment analysis were proteolysis, oxidation-reduction process, and homophilic cell adhesion via plasma membrane adhesion molecules; cellular components were extracellular region, membrane, and integral components of membrane; molecular functions were protein binding, calcium ion binding, and ATP binding (Supplementary Fig. S2). SVEP1 involved calcium ion binding and protein binding. The KEGG pathway annotations suggested that the transport and catabolism, signal transduction, neurodegenerative diseases, and immune system played a vital role in the disease. SVEP1 was annotated as fibrillins and related proteins containing Ca2+-binding EGF-like domains and classified in signal transduction mechanisms which was the most significant function classification in KOG analysis. In IPR annotations, the immunoglobulin V-set domain was most significant. In addition, SVEP1, the extracell protein, had the following characteristics: CUB and sushi domain-containing protein, IPR002035 (von Willebrand factor, type A), IPR000436 (Sushi/SCR/CCP domain), IPR000742 (EGF-like domain), IPR001881 (EGF-like calcium-binding domain), IPR013032 (EGF-like, conserved site), IPR001759 (Pentraxin-related), IPR003410 (HYR domain), and IPR011641 (Tyrosine-protein kinase ephrin type A/B receptor-like). Comparing XFG with XFS and ARC, KEGG enrichment analysis illustrated complement and coagulation cascades, D-glutamine and D-glutamate metabolism, inflammatory bowel disease, Th17 cell differentiation, proximal tubule bicarbonate reclamation, and staphylococcus aureus infection involved functional pathways, whereas malaria, staphylococcus aureus infection, intestinal immune network for IgA production, and systemic lupus erythematosus involved comparing XFG and XFS with ARC (Supplementary Figs. S3–S5). The thyroid or estrogen hormone and Alzheimer's disease might also involve in XFG. In GSEA analysis (Supplementary Fig. S6), the result was similar in IPR and serine proteases, the trypsin domain may play a vital role comparing XFG and XFS with ARC ($P < 0.05$). As for subcellular localization, the three most significant types were the extracell protein, the plasma membrane protein, and the cytoplasm protein. We built a PPI network to investigate the interactions between these DEPs (Supplementary Fig. S7). To predict key proteins in clusters 2 and 4, we used GOsemsim and found that none met with the cutoff value (> 0.75; Supplementary Fig. S8).

MR Analyses and Sensitivity Analysis

We performed an MR to verify the associations between proteins in clusters 2 and 4 and XFG. In phase I, we overlapped 16 pQTL in the deCODE cohort and our cohort and found 2 proteins (SVEP1 and HP) may be related to XFG in the primary analysis (Supplementary Table S6). There was a significant correlation between SVEP1 and XFG (OR = 1.20, 95% CI = 1.10 to 1.31, $P = 4.28 \times 10^{-5}$). We found that the SVEP1 in the DEPs had a robust result after quality control steps were conducted including MR-Egger, Simple-mode, Weighted median, and Weighted mode, whose beta was in the same direction and $P < 0.05$ in all methods (Fig. 4, Supplementary Fig. S9). Then, we repeated the process in another 2 cohorts and overlapped 8 pQTL in UKB-PPP and 7 pQTL in ARIC. We found that the association between SVEP1 and XFG remained significant (OR = 1.49, 95% CI = 1.01 to 2.19, $P < 0.05$ by IVW) in the ARIC cohort, whereas the HP was nonsignificant.

Investigative Ophthalmology & Visual Science

Table 2. Summary Based on Plasma/Serum Protein Assays

	Protein	Level	Sample	Method	Blood	Reference
1	Platelet Proteome	Down: Profilin-1 Up: P-selectin Nonsignificant: E-selectin and von Willebrand factor	29 XFS vs 42 healthy control vs 6 RVO	2D gel analysis, MALDI-TOF/TOF and Profilin-1 by Western blot analysis and P-selectin, E-selectin, and von Willebrand Factor by enzyme-linked immunosorbent assay	Plasma	Ugurel E, Narimanfar G, Cilek N, Kesim C, Altan C, Sahin A, and Yalcin O. (2024). Platelet proteome reveals novel targets for hypercoagulation in pseudoexfoliation syndrome. International Journal of Molecular Sciences, 25(3), 1403, https://doi.org/10.3390/ijms25031403.
2	Circulating autoantibodies	Down: HTRA2 antibodies and CLTA/B/C autoantibodies Up: HSP27 and CRYGS autoantibodies	45 XFG vs 31 NTG vs 43 POAG vs 46 control	Protein microarray	Serum	Beutgen V. M., Pfeiffer N., and Grus, F. H. (2021). Serological Levels of Anti-clathrin Antibodies Are Decreased in Patients With Pseudoexfoliation Glaucoma. Frontiers in immunology, 12, 616421, https://doi.org/10.3389/fimmu.2021.616421.
3	Klotho	Down	20 XFG vs 19 XFS vs 18 POAG vs 20 control	Enzyme-linked immunosorbent assay	Serum	Tokuc, E. O., Yuksel, N., Kır, H. M., and Acar, E. (2021). Evaluation of serum and aqueous humor klotho levels in pseudoexfoliation syndrome, pseudoexfoliation and primary open-angle glaucoma. International ophthalmology, 41(7), 2369–2375, https://doi.org/10.1007/s10792-021-01790-5.
4	Copper chaperone for superoxide dismutase	Down	70 XFS vs 70 ARC	Enzyme-linked immunosorbent assay	Plasma	Jing, Q., Li, D., Gao, W., Zhang, F., Lu, Y., and Jiang, Y. (2020). Associations of polymorphisms in LOXL1 and copper chaperone genes with pseudoexfoliation-syndrome-related cataract in a Chinese Uygur population. International ophthalmology, 40(7), 1841–1848, https://doi.org/10.1007/s10792-020-01354-z.
5	Netrin-1	Down	17 XFG and 29 XFS vs 47 cataract	Enzyme-linked immunosorbent assay	Serum	Okutucu, M., Findik, H., Aslan, M. G., and Arpa, M. (2020). Is Netrin-1 Deficiency Responsible for Inflammation and Systemic Diseases Related to Pseudoexfoliation?. Journal of glaucoma, 29(11), 1077–1081, https://doi.org/10.1097/IJG.0000000000001624.
6	YKL-40	Nonsignificant	24 XFS without glaucoma vs 20 ARC	Enzyme-linked immunosorbent assay	Serum	Gonen, T., Guzel, S., and Keskinbora, K. H. (2019). YKL-40 is a local marker for inflammation in patients with pseudoexfoliation syndrome. Eye (London, England), 33(5), 772–776, https://doi.org/10.1038/s41433-018-0308-8.
7	Thyroid stimulating hormone (TSH), free triiodothyronine (fT3), free thyroxine (fT4), c-reactive protein (CRP), and hemoglobin	Nonsignificant	29 XFG vs 77 POAG and 33 control	Automated Roche Diagnostic Cobas 8000 machine	Serum	Atalay, K., Savur, F. G., Kirgiz, A., Kaldırım, H. E., and Zengi, O. (2019). Serum levels of thyroid hormone, vitamin D, vitamin B12, folic acid, C-reactive protein, and hemoglobin in Pseudoexfoliation and primary open angle Glaucoma. Journal francais d'ophtalmologie, 42(7), 730–738, https://doi.org/10.1016/j.jfo.2019.01.002.

Table 2. Continued

	Protein	Level	Sample	Method	Blood	Reference
8	Decorin and tenascin C	Up	30 XFS vs 30 cataract	Enzyme-linked immunosorbent assay	Serum	Oruc, Y., Keser, S., Yusufoglu, E., Celik, F., Sahin, İ., Yardim, M., and Aydin, S. (2018). Decorin, Tenascin C, Total Antioxidant, and Total Oxidant Level Changes in Patients with Pseudoexfoliation Syndrome. Journal of ophthalmology, 2018, 7459496, https://doi.org/10.1155/2018/7459496.
9	High-sensitive C-reactive protein	Nonsignificant	59 XFS	CRP kit Roche (Roche Co, Basel/Kaiseraugst, Switzerland)	Serum	Jonas, J. B., Wei, W. B., Xu, L., and Wang, Y. X. (2018). Systemic inflammation and eye diseases. The Beijing Eye Study. PloS one, 13(10), e0204263, https://doi.org/10.1371/journal.pone.0204263.
10	C-reactive protein	Nonsignificant	96 XFS vs 79 control	BN II System nephelometer (High-Sensitivity CRP; Siemens Healthcare Diagnostics, Deerfield, IL, USA)	Plasma	Lesiewska, H., Łukaszewska-Smyk, A., Odrowąż-Sypniewska, G., Krintus, M., Mańkowska-Cyl, A., and Malukiewicz, G. (2017). Chosen Vascular Risk Markers in Pseudoexfoliation Syndrome: An Age-Related Disorder. Journal of ophthalmology, 2017, 5231095, https://doi.org/10.1155/2017/5231095.
11	Fetuin-A	Nonsignificant	25 XFS without glaucoma vs 25 cataract	Enzyme-linked immunosorbent assay	Serum	Yuksel, N., Takmaz, T., Ozel Turkcu, U., Ergin, M., Altinkaynak, H., and Bilgihan, A. (2017). Serum and Aqueous Humor Levels of Fetuin-A in Pseudoexfoliation Syndrome. Current eye research, 42(10), 1378–1381, https://doi.org/10.1080/02713683.2017.1324629.
12	Klotho and Endothelin-1	Down: Klotho Up: Endothelin-1	15 XFG vs 15 XFS vs 15 cataract	Enzyme-linked immunosorbent assay	Serum	Ahoor, M. H., Ghorbanihaghjo, A., Sorkhabi, R., and Kiavar, A. (2016). Klotho and Endothelin-1 in Pseudoexfoliation Syndrome and Glaucoma. Journal of glaucoma, 25(12), 919–922, https://doi.org/10.1097/IJG.0000000000000553.
13	Adropin and hemoglobin A1c	Down: adropin Nonsignificant: hemoglobin A1c	35 XFS vs 35 control	Enzyme-linked immunosorbent assay	Plasma	Oğurel, T., Oğurel, R., Topuz, M., Örnek, N., and Örnek, K. (2016). Plasma adropin level in patients with pseudoexfoliation. International ophthalmology, 36(5), 737–742, https://doi.org/10.1007/s10792-016-0185-8.
14	The phenotypic distribution of high-density lipoprotein (HDL)-linked paraoxonase 1	Nonsignificant	31 XFG vs 32 NTG vs 40 control	Spectrophotometry and dual substrate method	Serum	Yilmaz, N., Coban, D. T., Bayindir, A., Erol, M. K., Ellidag, H. Y., Giray, O., Sayrac, S., Tekeli, S. O., and Eren, E. (2016). Higher serum lipids and oxidative stress in patients with normal tension glaucoma, but not pseudoexfoliative glaucoma. Bosnian journal of basic medical sciences, 16(1), 21–27, https://doi.org/10.17305/bjbms.2016.830.
15	C-reactive protein	Nonsignificant	74 XFS vs 49 control	BN II System nephelometer (N high-sensitivity CRP)	Plasma	Lesiewska, H., Malukiewicz, G., Mańkowska-Cyl, A., and Odrowąż-Sypniewska, G. (2016). Lipids and C-reactive protein as vascular risk markers in pseudoexfoliation syndrome. Acta ophthalmologica, 94(5), e380–e381, https://doi.org/10.1111/aos.12883.

Table 2. Continued

	Protein	Level	Sample	Method	Blood	Reference
16	Antithrombin III activity, protein C activity, free protein S activity, and activated protein C resistance	Nonsignificant	25 XFG vs 25 POAG vs 25 XFS vs 25 healthy control	Antithrombin III activity-AT III (chromogenic substrate assay; STA-AT III), protein C activity (synthetic chromogenic substrate method; STA-Protein C), and free protein S activity (immunoturbidimetric method; STA- Liatest Free Protein S) assays.	Serum	Sekeroglu, M. A., Irkec, M., Mocan, M. C., and Orhan, M. (2016). Hereditary Thrombophilic Factors in Glaucoma. Journal of glaucoma, 25(2), 203–207, https://doi.org/10.1097/IJG.0000000000000148.
17	Omentin	Down	24 XFS without glaucoma vs 20 healthy control	Enzyme-linked immunosorbent assay	Serum	Bucak, Y. Y., Tosun, M., Simavli, H., Önder, H. I., and Erdurmuş, M. (2016). Serum Levels of Omentin in Pseudoexfoliation Syndrome. Journal of glaucoma, 25(2), 145–148, https://doi.org/10.1097/IJG.0000000000000139.
18	Sera proteins by comparative proteomics	XFG vs control: Down: IGHG2 Up: VTN, FBLN1 XFG vs POAG: Down: Apolipoprotein A-IV, Complement C3, Transthyretin, Serotransferrin, Alpha-1 antitrypsin, Ficolin-3	45 XFG vs 53 POAG vs 51 control	ProteoMiner, two-dimensional fluorescent difference gel electrophoresis (2D-DIGE), MALDI-TOF/TOF, and nanoLC-MS-MS and enzyme-linked immunosorbent assay	Serum	González-Iglesias, H., Álvarez, L., García, M., Escribano, J., Rodríguez-Calvo, P. P., Fernández-Vega, L., and Coca-Prados, M. (2014). Comparative proteomic study in serum of patients with primary open-angle glaucoma and pseudoexfoliation glaucoma. Journal of proteomics, 98, 65–78, https://doi.org/10.1016/j.jprot.2013.12.006.
19	YKL-40	Up	40 XFS vs 40 control	Enzyme-linked immunosorbent assay	Serum	Türkyılmaz, K., Öner, V., Kırbas, A., Sevim, M. S., Sekeryapan, B., Özgür, G., and Durmus, M. (2013). Serum YKL-40 levels as a novel marker of inflammation and endothelial dysfunction in patients with pseudoexfoliation syndrome. Eye (London, England), 27(7), 854–859, https://doi.org/10.1038/eye.2013.92.
20	High-sensitivity C-reactive Protein and Tumor Necrosis Factor Alpha	Up	30 XFS vs 30 control	Enzyme-linked immunosorbent assay	Serum	Sorkhabi, R., Ghorbanihaghjo, A., Ahoor, M., Nahaei, M., and Rashtchizadeh, N. (2013). High-sensitivity C-reactive Protein and Tumor Necrosis Factor Alpha in Pseudoexfoliation Syndrome. Oman medical journal, 28(1), 16–19, https://doi.org/10.5001/omj.2013.04.
21	C-reactive protein	Nonsignificant	33 XFS vs 23 healthy control	Nephelometric assay	Serum	Mocan, M. C., Dikmetas, O., and Irkec, M. (2011). Serum C-reactive protein levels in exfoliation syndrome and exfoliative glaucoma. Eye (London, England), 25(10), 1383–1384, https://doi.org/10.1038/eye.2011.166.

Table 2. Continued

	Protein	Level	Sample	Method	Blood	Reference
22	Antibodies to: C6orf129; stathmin-like 4; transmembrane protein 9 domain family, member B; fibroblast growth factor receptor 3; cleft lip and palate transmembrane protein 1; EH-domain-containing protein 1; and eukaryotic translation elongation factor 2	Up	21 XFG vs 19 control	Protein macroarrays	Serum	Dervan, E. W., Chen, H., Ho, S. L., Brummel, N., Schmid, J., Toomey, D., Haralambova, M., Gould, E., Wallace, D. M., Prehn, J. H., O'Brien, C. J., and Murphy, D. (2010). Protein macroarray profiling of serum autoantibodies in pseudoexfoliation glaucoma. Investigative ophthalmology and visual science, 51(6), 2968–2975, https://doi.org/10.1167/iovs.09-4898.
23	High sensitivity C-reactive protein	Nonsignificant	26 XFG vs 31 XFS vs 25 control	Nephelometric method	Plasma	Yüksel, N., Pirhan, D., Altintaş, O., and Cağlar, Y. (2010). Systemic high-sensitivity C-reactive protein level in pseudoexfoliation syndrome and pseudoexfoliation glaucoma. Journal of glaucoma, 19(6), 373–376, https://doi.org/10.1097/IJG.0b013e3181bdb570.
24	Vascular endothelial growth factor	Up	15 XFG and 37 XFS vs 32 control	Enzyme-linked immunosorbent assay	Plasma	Borazan, M., Karalezli, A., Kucukerdonmez, C., Bayraktar, N., Kulaksizoglu, S., Akman, A., and Akova, Y. A. (2010). Aqueous humor and plasma levels of vascular endothelial growth factor and nitric oxide in patients with pseudoexfoliation syndrome and pseudoexfoliation glaucoma. Journal of glaucoma, 19(3), 207–211, https://doi.org/10.1097/IJG.0b013e3181aae93e.
25	Protein carbonyl	Up	29 XFS without glaucoma vs 27 ARC	Spectrophotometry	Serum	Yagci, R., Ersöz, I., Erdurmuş, M., Gürel, A., and Duman, S. (2008). Protein carbonyl levels in the aqueous humour and serum of patients with pseudoexfoliation syndrome. Eye (London, England), 22(1), 128–131, https://doi.org/10.1038/sj.eye.6702751.
26	Alpha-1-antitriypsin	Up	44 XFS vs 40 healthy control	Nephelometric method	Serum	Cumurcu, T., Ozyurt, H., Demir, H. D., and Yardim, H. (2008). Serum alpha-1-antitriypsin levels in patients with pseudoexfolative syndrome. Current eye research, 33(2), 159–162, https://doi.org/10.1080/02713680701861752.
27	Protein carbonyl	Up	50 XFS without glaucoma vs 55 healthy control	Spectrophotometry	Serum	Yağci, R., Gürel, A., Ersöz, I., Keskin, U. C., Hepşen, I. F., Duman, S., and Yiğitoğlu, R. (2006). Oxidative stress and protein oxidation in pseudoexfoliation syndrome. Current eye research, 31(12), 1029–1032, https://doi.org/10.1080/02713680601001319.

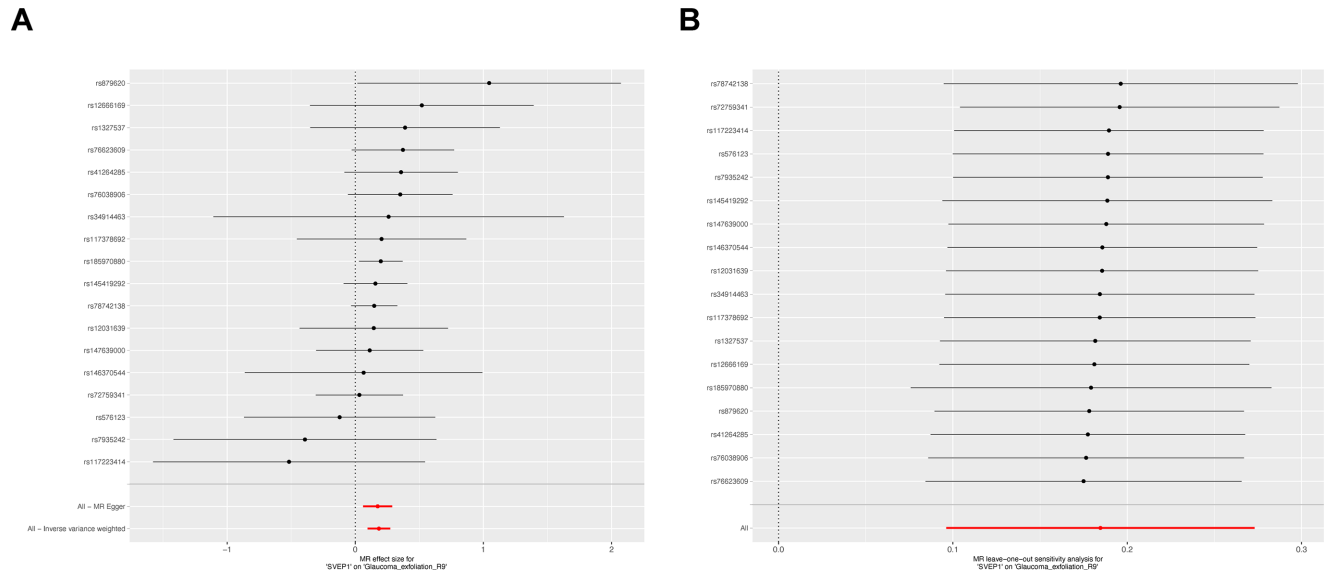

Figure 4. Mendelian randomization estimates for SVEP1 on XFG. (**A**) Forest plot. (**B**) Leave-one-out plot. MR = Mendelian randomization; SVEP1 = Sushi, von Willebrand factor type A, EGF and pentraxin domain containing 1; XFG = exfoliation glaucoma.

In phase II, we overlapped 13 pQTL in the deCODE cohort and previously reported plasma/serum proteins and found only endothelin 1 may have an impact on XFG in the primary analysis, which could not be found in UKB-PPP and ARIC (Supplementary Table S7). Besides, we performed the MR-Egger intercept and MR-PRESSO tests to identify potential pleiotropy and Cochran's Q tests to evaluate the heterogeneity (all $P > 0.05$). What's more, SVEP1 passed the leave-one-out analysis and Steiger filtering directionality test (see Fig. 4, Supplementary Table S8). The results of the sensitivity analysis guaranteed the association between SVEP1 and XFG. Then, we found that XFG was associated with SVEP1 (OR = 1.02, 95% CI = 1.00 to 1.04, $P = 0.02$ by IVW; see Supplementary Fig. S8, Supplementary Table S8) in reverse MR, whereas the result failed to pass through leave-one-out analysis (Supplementary Fig. S10). To determine whether protein SVEP1 involved the development of senile cataract, complicated cataract and POAG, or a reverse influence existed, we performed the two-sample bidirectional MR and found no potential influence existed between SVEP1 and these diseases (see Supplementary Table S8, Supplementary Figs. S11–S16).

Potential Pathway Between SVEP1 and XFG

To explore whether LOXL1-AS1 played a role in the effect of SVEP1 on XFG, we confirmed that LOXL1-AS1 had a protective role in XFG (OR = 0.66, 95% CI = 0.63 to 0.70, $P < 0.001$ by IVW, see Supplementary Table S8, Supplementary Fig. S17) and SVEP1 (OR = 0.99, 95% CI = 0.98 to 0.99, $P < 0.001$ by IVW; see Supplementary Table S8, Supplementary Fig. S18) by MR. After mediation analysis, we found LOXL1-AS1 had a protective role in XFG mediated by SVEP1 (mediated effect = −0.002, Z-score = −3.07, $P = 0.002$). In the cell level by RNA-sequencing, we validated that the expression of SVEP1 was elevated when LOXL1-AS1 was knocked down (fold change = 1.24, adjusted P value < 0.05; see Supplementary Table S9, Supplementary Fig. S19A), whereas there was no change when LOXL1-AS1 was overexpressed (fold change = 0.96, adjusted P value > 0.05; see Supplementary Table S9, Supplementary Fig. S19B).

Our previous study found that genus Senegalimassilia may influence XFG.[23] To explore the interaction between SVEP1 and genus Senegalimassilia, we performed two-sample bidirectional MR and found no associations between genus Senegalimassilia and SVEP1 in reverse MR (see Supplementary Table S8, Supplementary Fig. S20) and SVEP1 was associated with genus Senegalimassilia in forward MR (OR = 1.25, 95% CI = 1.01 to 1.55, $P = 0.04$ by IVW; see Supplementary Table S8, Supplementary Fig. S21), whereas the result failed to pass through the leave-one-out analysis.

Mendelian Randomization Phenome-Wide Association Study

We performed MR-PheWAS to identify the associations between SVEP1 with 3675 phenotypes. In addition, we found that 131 phenotypes in the UKB cohort and 262 phenotypes in the FinnGen cohort were suggested to be nominally significant, including alcohol-related diseases, congenital anomalies, infectious diseases, injuries and poisonings, mental disorders, neoplasms, pregnancy complications, sense organs, and dermatologic, digestive, endocrine/metabolic, genitourinary, musculoskeletal, neurological, hematopoietic, respiratory, or circulatory system problems (see Supplementary Table S10).

In the ocular area, SVEP1 was associated with ocular pain, Graves' disease, conjunctivitis, keratoconus, glaucoma, visual field defects, macular cyst, age-related macular degeneration (whether dry or wet), and diabetes retinopathy. In addition, in other areas, SVEP1 was associated with Alzheimer's disease or diseases including Alzheimer's disease, Parkinson's disease, immune bowel disease, hypertension or gestational hypertension, diabetes and its complications, hyperlipidemia, hypercholesterolemia, hemorrhagic disorder due to intrinsic circulating anticoagulants, diseases of white blood cells, aortic aneurysm, hernia, prolapse of

Investigative Ophthalmology & Visual Science

vaginal walls, genital prolapse, preeclampsia and eclampsia, peptic ulcer, and acanthosis nigricans. After multiple testing corrections, SVEP1 appeared to have an impact on glaucoma (OR = 1.14, 95% CI = 1.11 to 1.16, $P = 0.0000003$), diabetes insulin treatment (OR = 1.07, 95% CI = 1.06 to 1.09, $P = 0.000002$), diabetic ketoacidosis (OR = 1.15, 95% CI = 1.12 to 1.17, $P = 0.0000026$), and type 2 diabetes (OR = 1.07, 95% CI = 1.05 to 1.08, $P = 0.0000067$; see Fig. 1).

Discussion

We adopted a DIA-MS approach using in-depth plasma proteomics and pictured the largest wide-angled proteomic landscape mapping and identified deeper to identify comprehensive plasma proteome profiling of XFG/XFS. Plasma is the main clinical sample and is easy to obtain and standardize and is responsible for circulating proteins throughout the body that can reflect a variety of disease problems. However, plasma is the most complex and diverse sample in humoral analysis. The difference between the highest and lowest abundance protein concentrations in plasma is greater than 10 orders of magnitude, whereas the high-abundance proteins, such as albumin and immunoglobulin, account for 80% of the total plasma proteins, and the rest are present in very low concentrations, but they are associated with the evolution of many diseases and are potential biomarkers. Thus, we conducted this study by in-depth mass spectrometry technology to quantitatively identify proteins with high sensitivity and high accuracy.

With our proteomics data, our results suggested that infection, immune responses, including intestinal immune network, endocrine hormones, and complement and coagulation cascades, may be involved in the development of XFG. As the disease progressed, enrichment signals were biological pathways involved in the downregulation of anti-infection factors, upregulation of oxidative stress protein, and dysregulation of complement and coagulation cascades, and dysregulation of degradation of glutamine metabolism.

The past study that identified the most proteins identified 149 proteins and 17 studies focused only on one protein/peptide. There were six studies that found nonsignificant differences in C-reactive protein between XFG/XFS and the healthy controls and one found an increase in XFS. Our study found nonsignificant differences in C-reactive protein between the groups by DIA-MS and MR. In addition, our study also supported that endothelin 1 was related to XFG/XFS by MR.

We first found that high expression of SVEP1 was a risk factor for XFG and was validated in multiple large cohorts by the MR approach. This conclusion was robust across multiple ethnicities. In addition, SVEP1 was recently linked to coronary heart disease, blood pressure, dementia, and type 2 diabetes.[24–26] This may explain the onset of complications associated with XFG, such as cardiovascular disease and Alzheimer's disease. What's more, XFS was reported to be associated with a hernia and prolapse of the pelvic organs, and, in our results of MR-PheWAS, we validated these phenomena by SVEP1 at the nominal significance level.[27,28] The SVEP1 missense variant could be deleterious in TEK-related primary congenital glaucoma.[29] According to an open-angle glaucoma GWAS, rs61751937, a missense variant in SVEP1, could be pathogenic.[30] In our study, SVEP1 appeared to be related with diabetes and complications, revealing that SVEP1 is also a potential biomarker of diabetes or diabetes retinopathy. We need to validate this in further studies.

Plasma proteomics offers promising insights into pathogenesis and therapeutic opportunities. Our data triangulation and MR estimates integrating genetics, plasma protein levels, and diseases, indicate that SVEP1 may be a therapeutic target for XFG. We searched candidate drugs from a drug signatures' database for gene set analysis containing 22,527 gene sets (DSigDB, http://dsigdb.tanlab.org/DSigDBv1.0/).[31] We scanned DSigDB and found four potential candidate drugs based on computational drug signatures from the comparative toxicogenomics database. Cytarabine with the US Food and Drug Administration (FDA), the World Health Organization (WHO), Indian and China approval was predicted to decrease the expression of SVEP1; decitabine with the FDA's approval was predicted to decrease expression and reaction of SVEP1; cobaltous chloride was predicted to decrease the expression of SVEP1; and estradiol with the FDA, the WHO, Indian, China and Traditional Herbal approval was predicted to decrease SVEP1 and increase LOXL1. Estradiol is a naturally occurring hormone circulating endogenously in female subjects as an estrogen receptor agonist, causing an increase in hepatic synthesis of various proteins, which include sex hormone binding globulin and thyroid-binding globulin. However, SVEP1 expression is regulated in an estrogen-dependent manner, whereas 17beta-estradiol can increase the level of the SVEP1 expression.[32–34] In our study, downregulation of immunoglobulin anti-estradiol indicated that the function of estradiol to SVEP1 may increase. This suggested there may exist potential gender differences on XFG and the effects of female hormone fluctuations, such as menopause, may also have an impact on XFG. Further studies are needed to determine the sex difference in the onset of the disease caused by SVEP1. What's more, our results suggested SVEP1 expression might be regulated by LOXL1-AS1. The downregulation of LOXL1-AS1 and subsequent upregulation of SVEP1 expression were implicated in XFG pathogenesis. However, the primary protective function of LOXL1-AS1 may lie in other mechanisms. This study utilized mass spectrometry data to identify significant differential proteins and reinforced the conclusions by MR, but validation for the findings should be carried out in a large cohort population and further experiments are still needed to understand the effect of SVEP1 on XFG.

Acknowledgments

The authors thank the participants and investigators of the FinnGen, UK Biobank, deCODE, and the ARIC study for their important contributions. This work is supported by Extreme Smart Analysis platform (https://www.xsmartanalysis.com/).

Author Contributions: Study concept and design: H.W., G.X., and L.J. Acquisition, analyses, or interpretation: L.J., M.Y., X.L., Z.K., H.Y., M.X., Z.S., G.S., T.Y., M.G., A.M., Z.D., W.A., Z.X., T.C., W.W., H.W., and G.X. Drafting of the manuscript: L.J. Critical revision of the manuscript for important intellectual content: L.J., M.Y., X.L., Z.K., H.Y., M.X., Z.S., G.S., T.Y., M.G., A.M., Z.D., W.A., Z.X., T.C., W.W., H.W., and G.X. Statistical analyses: L.J. and Z.X. Obtained funding: G.X. Administrative, technical, or material support: H.W., G.X., and W.A. Study supervision: H.W. and G.X.

Supported by Guangdong Basic and Applied Basic Research Foundation (2022A1515012257), the Fundamental Research Funds of the State Key Laboratory of Ophthalmology, and an

award from Guangdong Provincial Department of Science and Technology (KTPYJ2022031).

Disclosure: **J. Li**, None; **Y. Ma**, None; **L. Xie**, None; **K. Zhuo**, None; **Y. He**, None; **X. Ma**, None; **S. Zheng**, None; **S. Guo**, None; **Y. Tang**, None; **G. Muhetaer**, None; **M. Aizezi**, None; **D. Zhang**, None; **A. Wumaier**, None; **X. Zhang**, None; **C. Tang**, None; **W. Wang**, None; **W. Huang**, None; **X. Gao**, None

References

1. Jayaram H, Kolko M, Friedman DS, Gazzard G. Glaucoma: now and beyond. *Lancet (London, England).* 2023;402(10414):1788–1801.
2. Kapuganti RS, Alone DP. Current understanding of genetics and epigenetics in pseudoexfoliation syndrome and glaucoma. *Mol Aspects Med.* 2023;94:101214.
3. Wang W, He M, Zhou M, Zhang X. Ocular pseudoexfoliation syndrome and vascular disease: a systematic review and meta-analysis. *PLoS One.* 2014;9(3):e92767.
4. Hirbo JB, Pasutto F, Gamazon ER, et al. Analysis of genetically determined gene expression suggests role of inflammatory processes in exfoliation syndrome. *BMC Genomics.* 2023;24(1):75.
5. Schmitt HM, Hake KM, Perkumas KM, et al. Lysyl oxidase-like 1-antisense 1 (LOXL1-AS1) lncRNA differentially regulates gene and protein expression, signaling and morphology of human ocular cells. *Hum Mol Genet.* 2023;32(21):3053–3062.
6. Deutsch EW, Omenn GS, Sun Z, et al. Advances and utility of the human plasma proteome. *J Proteome Res.* 2021;20(12):5241–5263.
7. Sanderson E, Glymour MM, Holmes MV, et al. Mendelian randomization. *Nat Rev Methods Primers.* 2022;2:6.
8. Ma J, Chen T, Wu S, et al. iProX: an integrated proteome resource. *Nucleic Acids Res.* 2019;47(D1):D1211–D1217.
9. Chen T, Ma J, Liu Y, et al. iProX in 2021: connecting proteomics data sharing with big data. *Nucleic Acids Res.* 2022;50(D1):D1522–D1527.
10. Yu G, Li F, Qin Y, Bo X, Wu Y, Wang S. GOSemSim: an R package for measuring semantic similarity among GO terms and gene products. *Bioinformatics.* 2010;26(7):976–978.
11. Ferkingstad E, Sulem P, Atlason BA, et al. Large-scale integration of the plasma proteome with genetics and disease. *Nat Genet.* 2021;53(12):1712–1721.
12. Sun BB, Chiou J, Traylor M, et al. Plasma proteomic associations with genetics and health in the UK Biobank. *Nature.* 2023;622(7982):329–338.
13. Zhang J, Dutta D, Köttgen A, et al. Plasma proteome analyses in individuals of European and African ancestry identify cis-pQTLs and models for proteome-wide association studies. *Nat Genet.* 2022;54(5):593–602.
14. Võsa U, Claringbould A, Westra H-J, et al. Large-scale cis- and trans-eQTL analyses identify thousands of genetic loci and polygenic scores that regulate blood gene expression. *Nat Genet.* 2021;53(9):1300–1310.
15. Kurilshikov A, Medina-Gomez C, Bacigalupe R, et al. Large-scale association analyses identify host factors influencing human gut microbiome composition. *Nat Genet.* 2021;53(2):156–165.
16. Wang J, Kurilshikov A, Radjabzadeh D, et al. Meta-analysis of human genome-microbiome association studies: the MiBioGen consortium initiative. *Microbiome.* 2018;6(1):101.
17. Kurki MI, Karjalainen J, Palta P, et al. FinnGen provides genetic insights from a well-phenotyped isolated population. *Nature.* 2023;613(7944):508–518.
18. Canela-Xandri O, Rawlik K, Tenesa A. An atlas of genetic associations in UK Biobank. *Nat Genet.* 2018;50(11):1593–1599.
19. Ge Y-J, Ou Y-N, Deng Y-T, et al. Prioritization of drug targets for neurodegenerative diseases by integrating genetic and proteomic data from brain and blood. *Biol Psychiatry.* 2023;93(9):770–779.
20. Schmitt HM, Johnson WM, Aboobakar IF, et al. Identification and activity of the functional complex between hnRNPL and the pseudoexfoliation syndrome-associated lncRNA, LOXL1-AS1. *Hum Mol Genet.* 2020;29(12):1986–1995.
21. Gagliano Taliun SA, VandeHaar P, Boughton AP, et al. Exploring and visualizing large-scale genetic associations by using PheWeb. *Nat Genet.* 2020;52(6):550–552.
22. Sjöstedt E, Zhong W, Fagerberg L, et al. An atlas of the protein-coding genes in the human, pig, and mouse brain. *Science.* 2020;367(6482):eaay5947.
23. Li J, Ma X, Zhuo K, et al. Investigating the uncertain causal link between gut microbiota and glaucoma: a genetic correlation and Mendelian randomisation study. *Clin Exp Ophthalmol.*2024;52(9):945–956.
24. Stitziel NO, Stirrups KE, Masca NGD, et al. Coding variation in ANGPTL4, LPL, and SVEP1 and the risk of coronary disease. *N Engl J Med.* 2016;374(12):1134–1144.
25. Emilsson V, Gudmundsdottir V, Gudjonsson A, et al. Coding and regulatory variants are associated with serum protein levels and disease. *Nat Commun.* 2022;13(1):481.
26. Walker KA, Chen J, Zhang J, et al. Large-scale plasma proteomic analysis identifies proteins and pathways associated with dementia risk. *Nat Aging.* 2021;1(5):473–489.
27. Besch BM, Curtin K, Ritch R, Allingham RR, Wirostko BM. Association of exfoliation syndrome with risk of indirect inguinal hernia: the Utah Project on Exfoliation Syndrome. *JAMA Ophthalmol.* 2018;136(12):1368–1374.
28. Li Y, Wu B, An C, et al. Mass cytometry and transcriptomic profiling reveal body-wide pathology induced by Loxl1 deficiency. *Cell Prolif.* 2021;54(7):e13077.
29. Young TL, Whisenhunt KN, Jin J, et al. SVEP1 as a genetic modifier of TEK-related primary congenital glaucoma. *Invest Ophthalmol Vis Sci.* 2020;61(12):6.
30. Gharahkhani P, Jorgenson E, Hysi P, et al. Genome-wide meta-analysis identifies 127 open-angle glaucoma loci with consistent effect across ancestries. *Nat Commun.* 2021;12(1):1258.
31. Yoo M, Shin J, Kim J, et al. DSigDB: drug signatures database for gene set analysis. *Bioinformatics.* 2015;31(18):3069–3071.
32. Shur I, Zemer-Tov E, Socher R, Benayahu D. SVEP1 expression is regulated in estrogen-dependent manner. *J Cell Physiol.* 2007;210(3):732–739.
33. Glait-Santar C, Benayahu D. SVEP1 promoter regulation by methylation of CpG sites. *Gene.* 2011;490(1–2):6–14.
34. Glait-Santar C, Benayahu D. Regulation of SVEP1 gene expression by 17β-estradiol and TNFα in pre-osteoblastic and mammary adenocarcinoma cells. *J Steroid Biochem Mol Biol.* 2012;130(1–2):36–44.